

# A RESONANCE STUDY OF IMPEDANCE BASED STRUCTURAL HEALTH MONITORING

Pablo A. Tarazaga, Daniel M. Peairs, and  
Daniel J. Inman

Center for Intelligent Material Systems and  
Structures  
Virginia Polytechnic Institute and State  
University  
310 Durham Hall (Mail code 0261)  
Blacksburg, VA 24061-0261, USA

## Abstract

Impedance-based structural health monitoring uses collocated piezoelectric transducers to locally excite a structure at high frequencies. The response of the structure is measured by the same transducer. Changes in this response indicate damage. Frequency range selection for monitoring with impedance-based structural health monitoring has, in the past, been done by trial and error methods, or been selected after analysis by engineers familiar with the method. For future applications it is desirable to be able to automatically select frequency ranges, perhaps even before installing the system. In this study, analysis of the measurement change through a damage metric is examined and related to characteristics of the measurement. Specifically, an outlier detection framework was used to statistically evaluate the sensing ability of the transducers at various frequency ranges. The variation in undamaged measurements is compared to the amount of change in the measurement upon various levels of damage. Testing was performed with both solid piezoceramic transducers and macro-fiber composite (MFC) piezoelectric devices of different sizes bonded to aluminum and fiber reinforced composite structures. The results indicate that frequency ranges containing a resonance of the actuator are more suited for structural health monitoring.

## Introduction

The ability of piezoelectric materials to act as sensors and actuators has led to the development of structural health monitoring (SHM) systems that rely on the local and

active interrogation of a structure. One such system is electromechanical impedance-based structural health monitoring. Impedance-based SHM is a developing method for monitoring structures. The basic concept of the impedance method is to use high frequency vibrations (30-300 kHz) to monitor the local area of a structure for changes in structural impedance. These changes would indicate damage or imminent damage. This is possible using piezoelectric sensor/actuators bonded to the structure, causing their electrical impedance to be directly related to the structure's mechanical impedance. The electrical response is analyzed where, since the presence of damage causes the response of the system to change, damage is shown as a phase shift or magnitude change in the measured response.

Although, a significant body of research has been developed about impedance-base SHM, the technique is still not developed enough to be a "plug-n-play", "slap-on" or automatically installed, monitoring system. The method still generally requires personnel familiar with impedance-based structural health monitoring to select parameters of the system to be able to reliably detect small amounts of damage on a structure. The research presented in this paper addresses the frequency range selection of impedance measurements used for SHM. Two experimental structures are used to examine frequency range selection. The frequency ranges with resonances of the actuator are compared to frequency ranges without. The results indicate that the ranges with the sensor/actuator resonances are better for monitoring with the impedance-based method.

## Principles of Impedance-based Structural Health Monitoring

The impedance-based health monitoring method is made possible through the use of piezoelectric patches (most often lead zirconate titanate, PZT) bonded to the structure that act as both sensors and actuators on the system. When a piezoelectric is stressed it produces an electric charge. Conversely when an electric field is applied the piezoelectric produces a mechanical strain. The patch is driven by a sinusoidal voltage sweep. Since the patch is bonded to the structure, the structure is deformed along with it and produces a local dynamic response to the vibration. The area that one patch can excite depends on the structure configuration and material. The response of the system is transferred back from the piezoelectric patch

as an electrical response. The electrical response is then analyzed where, since the presence of damage causes the response of the system to change, damage is shown as a phase shift or magnitude change in the impedance. A more detailed explanation of the technique can be found in the references [1-4].

Impedance-based SHM has been tested successfully on many laboratory structures [4-7], as well as a few *in situ* applications [8,9]. The impedance method has many advantages compared to global vibration based and other damage detection methods. The principal advantages of the impedance approach compared to other techniques are the following [4]:

- The technique is not based on any model, and thus can be easily applied to complex structures.
- The technique uses small non-intrusive actuators to monitor inaccessible locations.
- The sensor (PZT) exhibits excellent features under normal working conditions, has a large range of linearity, fast response, light weight, high conversion efficiency and long term stability.
- The technique, because of high frequency, is very sensitive to local minor changes.
- The measured data can be easily interpreted.
- The technique can be implemented for on-line health monitoring.
- Low excitation forces (usually less than 1 V) produce power requirements in the range of microwatts, making the method an ideal candidate to be run by a self powered system.

Typically, the impedance method uses a damage metric to summarize and quantify the comparison of the frequency response functions from the impedance measurements. Common damage metrics include the root mean square deviation (RMSD), 1- the cross correlation coefficient and damage metrics related to these. In this study the cross correlation coefficient is used, however the procedures could be applied to other damage metrics.

In a monitoring framework, if the damage metric is larger than a user specified level, then the structure is said to be damaged. This level can be set using the method of outlier detection.

If the data comes from a normal distribution and the number of measurements is large, a simple Z statistic may be used. Also, if the data comes from a non-skewed distribution, the t-statistic can be used even for small data sets (population variance unknown). Alternatively, some researchers have concluded that the damage sensitive features in SHM systems will follow an extreme value distribution [10]. In this case, several different procedures may be used, including: the Box-Cox transformation for transforming Weibull data to a normal distribution, the Wilcoxon test, or tests on the median. The probability (p-value) of a measurement may also be calculated if the population distribution is known. Todd et al. [11] concluded that outlier detection methods, or more specifically, the frequency of outliers, while good for detecting damage, are not a good method of classifying levels of damage since the percentage of outliers saturates quickly once the structure is damaged.

Several past studies have examined the selection of appropriate frequency ranges for impedance-based SHM. A suitable frequency range depends on the structure being used and type of damage to be detected. The frequency range selected should have many peaks, since this indicates that there is a large amount of structural information. [4,5]. Often several frequency ranges that show many peaks are monitored. Historically, the frequency range has been determined through trial and error. Gyekenyesi et al. [12] performed a good study on frequency range selection for impedance measurements that identified frequency ranges with low variability. Unfortunately, the sensitivity to damage of each frequency range was not taken into account. They also did not associate the regions with the best response to features of the impedance measurement so that future researchers would not need to perform the same study as theirs. Simmers [13] has reported results of sensitivity tests for frequency range selection. In several studies, corrosion damage was simulated on structures using small amounts of wax and the frequency ranges with the highest sensitivity were selected for monitoring. In one study of induced corrosion, the variation of the frequency range was taken into account as well by subtracting a confidence interval from the damage metric. Resulting positive values deemed the frequency range acceptable for monitoring. The detection trend was not consistent for different sensors and proximities to the damage nor was detectability related to features of the impedance measurement.

In addition to having high peak density and low noise, in order to ensure that damage can be “seen”, the wavelength of the excitation signal must be smaller than the characteristic length of the damage [14]. However, at frequency ranges high enough to produce wavelengths that can detect small amounts of damage, the characteristics of the sensor/actuator itself may have an effect on the ability to detect damage. Specifically, resonances of the piezoelectric sensor/actuator often cause large peaks in the impedance signature, as well as an increase in modal density near the resonance, which may affect the sensing abilities at those frequencies.

### Experimental Investigation

In order to investigate the effect of the active sensor resonances on sensing ability, experiments were performed on two structures, an aluminum beam, and a composite boom. The composite was expected to exhibit higher damping and thus a more localized sensing area. PZT’s were used as actuators in the aluminum beam experiment and macro-fiber composites (MFC), which could conform to a curved shape, were used in the composite boom experiments.

#### Aluminum Beam Experiment

In the first experiment, two different sized PZT patches were attached to opposing sides of a 121.92 x 3.175 x .635 cm aluminum beam as seen in Fig. 1. The dimensions of PZT 1 and PZT 2 measure 1.27 x 2.54 cm and 3.83 x 2.54 cm respectively. Both PZT’s are Piezo Systems, Inc. material PSI - 5H4E, 0.267 mm thick, bonded to the base structure with cyanoacrylate, with copper tape protruding from underneath to provide for electrical connection. Before bonding, the impedance of each PZT was measured in its free condition from 0.1 to 200 kHz in 20 Hz intervals. Electrical connection was made by attaching copper tape with conductive adhesive to both electrodes of the PZT. The resulting impedances are shown in Fig. 2.



Figure 1. a) PZT 1, b) PZT 2 (attached to same end, opposite side of beam).

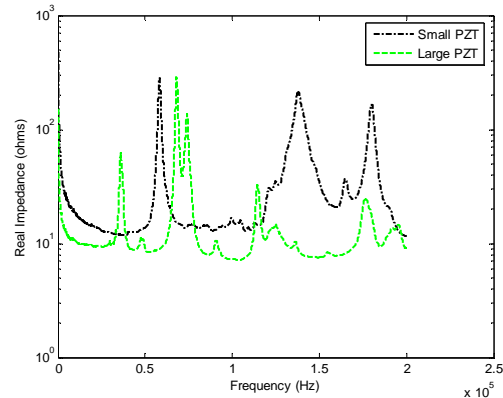


Figure 2. Impedance response of unbonded PZTs.

Once the PZTs were bonded, a series of baseline measurements were made over a period of several days with each PZT again from 0.1 to 200 kHz in 20 Hz steps. A 12 gram magnet was then attached to each side of the beam (25 g total), as a simulation of damage, approximately 70.5 cm from the end with the PZTs and the impedance measured in the damage state.

In order to determine how well different frequency ranges for each PZT can detect the damage, the baseline data was averaged to form a single baseline impedance measurement. The data was then analyzed in 8 kHz intervals. Each baseline measurement was compared to the average baseline using the maximum cross correlation between the baseline and damaged measurement for that frequency range as a damage indicator. The correlation was subtracted from 1 to make the comparison consistent with other damage metrics (increasing damage causes an increase in the metric). This damage metric is insensitive to shifting and scaling of the measurements, making it idea for comparing measurements between two PZTs and at different frequency ranges. The damage metrics for all baseline measurements were then averaged and the standard deviation calculated for each frequency range. For this test the damage metric values were assumed to be normally distributed. A plot of the average baseline damage metric and standard deviations for each PZT is shown in Fig. 3 and 4.

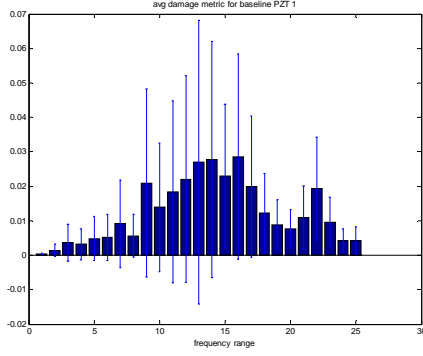


Figure 3. PZT 1 baseline damage metric.

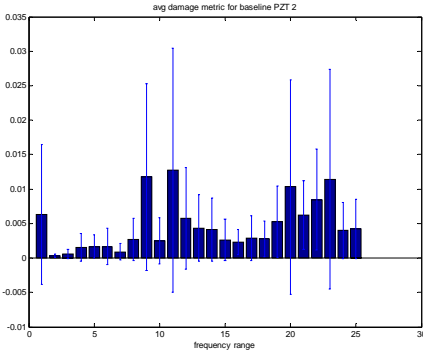


Figure 4. PZT 2 baseline damage metric.

The metrics for the damaged case were then calculated and compared to the baseline metrics using hypothesis testing for outlier analysis. To test if the mean of the new sample is larger than the mean of the baseline the following hypothesis test is constructed:

$$H_0 : \mu = \mu_0$$

$$H_1 : \mu \geq \mu_0$$

where  $\mu$  is the sample mean and  $\mu_0$  is the population mean, in this case, the mean of the baseline damage metric. The test statistic,  $Z_0$ , was calculated for each frequency range using the following equation,

$$Z_0 = \frac{\bar{X} - \mu_0}{\sigma / \sqrt{n}}$$

where  $\bar{X}$  is the sample mean and  $n$  is the number of samples. In this case,  $\bar{X}$  is the value of the damaged metric,  $n$  is 1 since only one sample is being compared, and  $\mu_0$  and  $\sigma$  are the baseline mean and standard deviation. This tests whether the mean of the new measurement is the same or greater (using a one sided test) than the mean of the baseline measurements based on a given confidence level. If  $H_0$  is true the probability is at least  $1-\alpha$

that the test statistic,  $Z_0$  is less than  $Z_\alpha$ . In this example  $\alpha$  is chosen to be 0.01 so that if  $Z_0$  is less than 2.33, there is a 99% probability that the mean of population has not changed. Again, in this study, the distribution of damage metrics for a PZT at a given frequency range is assumed to be normal and the baseline measurements are assumed to accurately represent the mean and deviation of the population. For testing on an actual structure, extreme value distributions (Weibull, Gumbel or Frechet) may be a better candidate distribution. However, since this study only aims to compare the ability of two PZT's to sense damage on the same structure, the more common normal distribution was used.

The resulting  $Z_0$  values, along with the average baseline measurements and unbonded measurements for PZTs 1 and 2 are shown in Fig. 5. As can be seen in the first two plots of the baseline impedance signatures with unbonded impedance signatures, the resonance frequencies of the PZT do not change significantly when bonded. Focusing on plot c., as expected it is shown that the impedance signatures are much more sensitive at low frequencies to the added mass than at high frequencies. In addition, the large PZT does a better job at detecting the damage than the smaller, since it can more effectively excite the beam. Also, comparing the height of the  $Z$  statistic at different frequencies seems to indicate the PZT resonances have a diminishing effect on the sensing ability of the large PZT. Plot d. compares the sensing ability of the PZTs at each frequency range. Although, the larger PZT does a better job of sensing the damage than the smaller PZT, at a few frequencies, the small PZT does just as well, or better than the large PZT. This is indicated by the ratio of the  $Z$  statistic being equal to or larger than 1.0. These frequencies seem to occur in most cases just after the peaks in the small PZT unbonded response. The PZT resonances are not clearly visible in the bonded response, however, a small shift to higher frequencies is expected due to the stiffening effects of bonding. The optimum testing frequencies occur where the PZT resonance is expected to be.

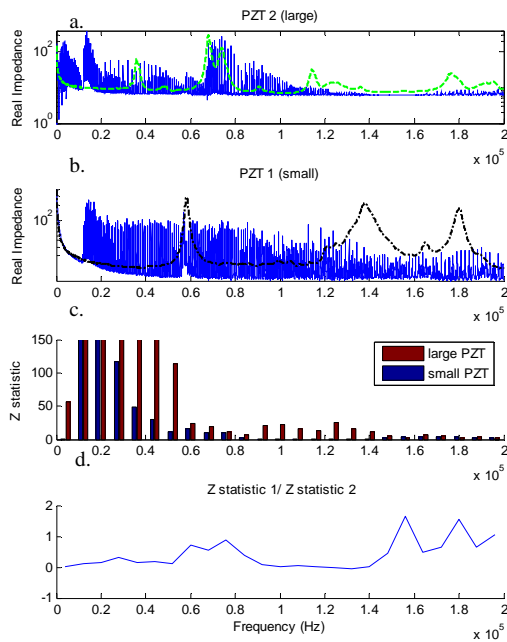


Figure 5 a. Baseline and unbonded impedance of PZT 2. b. Baseline and unbonded impedance of PZT 1. c. Z statistic for PZT 1 and 2 for added mass. d. Ratio of Z statistics for added mass.

A second test was carried out to further investigate the sensing ability of the two PZTs. In order to reduce the low frequency sensing ability of each PZT, an additional baseline measurements was made with increased mass variability. A small mass of approximately 2 g was attached to the beam for one of the baseline measurements. In addition, the damage was changed from an added mass to a 1 mm wide quarter width cut. The average damage metric for PZT 1 with the increased mass variability is shown in Fig. 6. The increase in variability is mostly in the lower frequency ranges. This highlights one of the benefits of high frequency methods, that they are less sensitive to boundary condition changes.

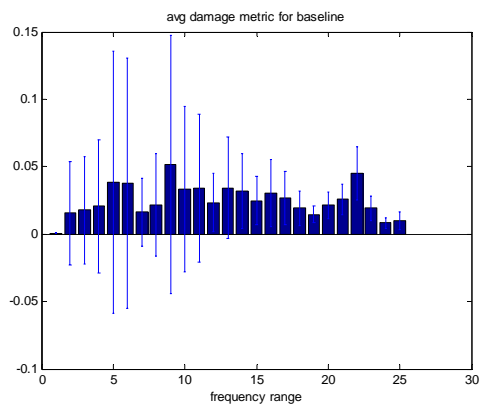


Figure 6. Average baseline for PZT 1 (small) with increased mass variability.

Results from this experiment are shown in Fig. 7. Again, baseline and unbonded measurements are included for reference. It can be seen again that lower frequencies are not as responsive to the damage in this case because of the added mass variability. In addition, the small PZT is relatively more sensitive than in the previous case. The higher frequencies, however, react similarly to the damage. Again, the data indicates that the regions just after the unbonded PZT resonances should have the best sensing ability as test frequency ranges. This emphasizes the importance of investigating the entire frequency range of impedance-based SHM as opposed to just randomly choosing a frequency range. However, frequencies without a PZT resonance can still detect damage, and may be more efficient at detecting far away damage because of the greater excitation ability at resonance.

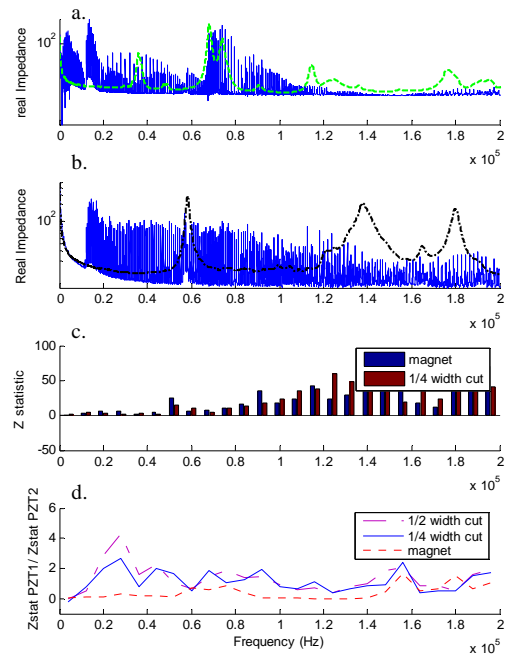


Figure 7. a. Baseline and unbonded impedance of PZT 2. b. Baseline and unbonded impedance of PZT 1. c. Z statistic for PZT 1 for quarter width cut and magnet. d. Ratio of Z statistics.

### Composite Boom Experiment

The second structure examined is a composite boom for use in a space reflector. It is envisioned that such structures could be made by inflating and then rigidizing them once they have reached orbit. The specific boom used in this study is a thermoplastic resin system rigidizeable boom provided by ILC Dover Inc.

Previous work has investigated the impedance method's ability to monitor composites. Pohl

et al. [15] induced damage on carbon fiber reinforced polymers and detected it by monitoring changes in the impedance peaks. Identification of delamination in composites was done by Bois and Hochard [16] using the impedance method. Research by Grisso et al. [17,18] shows the feasibility of detecting cracks in cross-ply graphite/epoxy composites using PZT and the impedance method. Some preliminary work has also been presented in Tarazaga et al. [19] concerning an inflatable rigidizable boom where damage was simulated by mass loading and the impedance method was used to detect changes.

Commercially available Macro-Fiber Composite (MFC) [20] piezocomposite devices are used as transducer elements in this study. Piezoelectric composite devices, such as active fiber composites (AFC) [21] or MFC, are flexible and conformable. This permits them to be integrated easily into or on curved structures. They also have high actuation performance and durability, compared with monolithic piezoceramic plates or wafers, and possess orthotropic mechanical and piezoelectric properties, which can be useful in optimizing their structural actuation and sensing performance [22]. MFC piezoelectric composite actuators have also been successfully integrated within space rigidized composite booms in several previous studies at NASA Langley Research Center [23-25].

Two sizes of MFC devices are used. The ability of the impedance method to detect actual perforations in the structure such as those caused by impacting meteorites or orbital debris (MMOD) is assessed. These perforations potentially could occur in pairs, i.e., with an initial entry hole and a path-dependant exit hole. Previous investigations have looked at detecting and assessing the size of hole damage and location from the collocated sensors [26], where as, the current investigation focuses on frequency range selection.

The experiments were conducted using an untapered, cylindrical, inflatable-rigidizable composite boom. The boom structure consisted of two 0/90 carbon fiber plies consolidated with a proprietary space-rigidizeable thermoplastic resin system. All testing was performed at room temperature where the thermoplastic resin system is below its designed glass transition temperature, and the structure is in its rigid phase. The boom was 1.73 m long by 97.8 mm in outer diameter. Net wall thickness was 0.61 mm though this

varied significantly. Holes in the boom already existed in some locations where the fiber tows did not form a close mesh.

The boom was suspended from the ceiling to provide a free-free mechanical boundary configuration. Two commercially manufactured MFC actuators (Smart Material Corporation, Sarasota, FL) were installed near one end of the boom on opposite sides of the structure using epoxy. All electrical impedance measurements were taken using an HP 4194A impedance analyzer. The experimental setup, including the arrangement and dimensions of the MFC devices, is shown in Fig. 8.

Simulated micrometeorite damage was applied to the structure by hand-drilling holes of various diameters into the boom wall. The holes were applied in pairs to simulate MMOD strikes with entry and possible exit perforations. Hole diameters ranged from 0.79 mm to 4.76 mm, and were drilled in three regions of the structure: at the midpoint of the beam, at  $\frac{1}{4}$  the length of the beam away from the sensors, and at the end of the beam farthest from the sensors. Fig. 9 shows the regions chosen for the test.

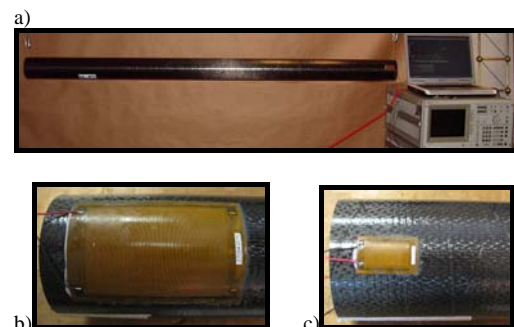


Figure 8. (a) Suspended boom configuration and HP 4194A Impedance analyzer used for testing and (b) close up pictures of large MFC (109 mm x 73.7 mm) used as collocated sensor/actuator (c) close up picture of small MFC (31.8 mm x 25.4 mm) used as collocated sensor/actuators.



Figure 9. Boom Schematic.

A series of at least 12 baselines consisting of 12400 frequency points each were made with each MFC over a frequency range of 0.1 kHz to 248.08 kHz (20 Hz steps). A sample impedance measurement for each sensor is shown in 10. The baselines were taken over several days to account for the possibility of variations caused by fluctuations in the

laboratory temperature and relative humidity. The measurements were all taken in sets of three consecutive measurements by an automated control program for the impedance analyzer.

The data is divided into 31 frequency ranges consisting of 401 data points for analysis. Each frequency range is 8 kHz wide. Throughout the analysis each frequency range is treated independently. In addition, a new set of baseline data was measured before damage was introduced at a new location. This generates 186 data sets for the current testing. The baseline measurements are averaged at each frequency range. The damage metric is then calculated for each baseline measurement by comparing it to the average baseline. The mean and standard deviation of the damage metrics for each frequency range is calculated. Examples of the average baseline damage metric for the large and small MFC's are shown in Fig. 11 and 12. The level of the average baseline damage metric was consistent for each set of baseline measurements made for each damage location. Additionally, higher baseline metrics also have higher variability.

As simulated MMOD damage is applied to the boom, the damage metric for each succeeding measurement is calculated and then compared to the average baseline measurement. Example trends in damage metrics with increasing hole diameter are shown for the large MFC's response in Figure 13. Metrics shown are for the 128.1 to 136.1 kHz frequency range and the 192.1 to 200.1 kHz frequency range.

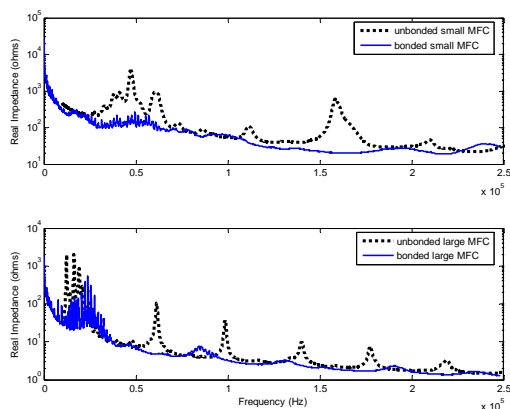


Figure 10. Sample baseline impedance measurements (real part) for large and small MFC on composite boom.

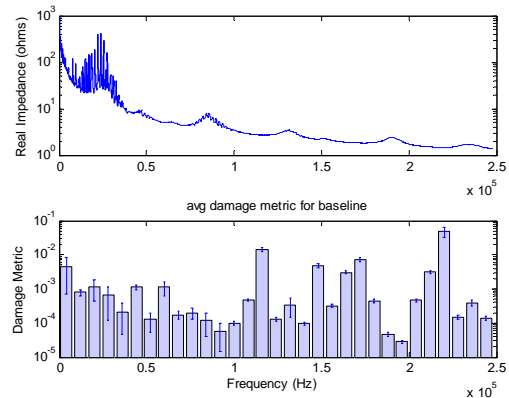


Figure 11. Average baseline damage metric for large MFC, with baseline measurement shown for comparison.

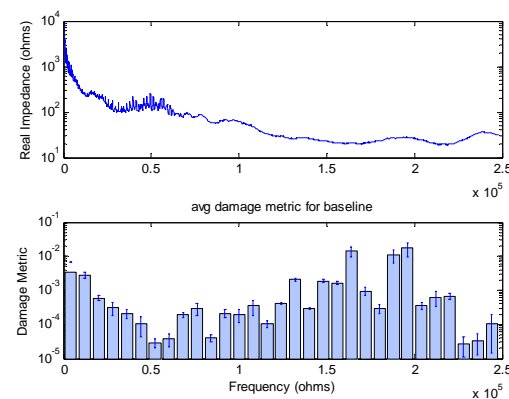


Figure 12. Average baseline damage metric for small MFC, with baseline measurement shown for comparison.

The damage metrics were analyzed using the same method as was used on the aluminum beam testing. In this case though, since multiple measurements were made for one damage level, the number of degrees of freedom in the test statistic was increased to three. This may be too large of an increase because the assumption of independent data is questionable since the measurements were made consecutively in groups of three. Taking the data consecutively causes each measurement in a group of three to be acquired with approximately the same environmental conditions (temperature and humidity) compared to the overall environmental variability. This causes clustering which causes the confidence intervals of the data to be too narrow [27] and ultimately the test statistic to indicate damage more strongly than is actually measured. These effects can be corrected by reducing the degrees of freedom in the calculated test statistic. Since the actual degrees of freedom is not known the number of degrees of freedom are conservatively kept at 1 for the calculation of the test statistic. Variance of the sample being tested is assumed to be the same as the variance of the baseline

measurements. This allows inferences to be made using a single population's characteristics rather than two different populations.

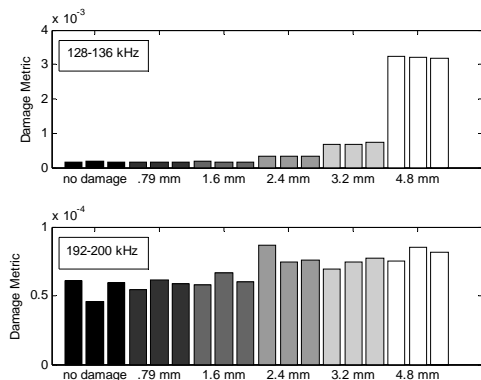


Figure 13. Damage metric of large MFC at 128-136 kHz and 192-200 kHz, for increasing levels of damage at the midpoint of the boom.

The frequency ranges that contain resonances of the MFC sensor are more sensitive to the damage than frequency ranges that are flat. Also, the largest increases in damage metric from one damage level to the next are for the largest holes. This may indicate that the damage metric is sensitive to the total area of the damage rather than just diameter of the hole. It should also be noted that the frequency ranges that increase more for the large damage also increase more for the smaller damage. In general, the higher frequencies that are sensitive to damage have a greater distinction between the levels of damage. Finally, several frequency ranges indicate damage when in fact there is none. If the mean value of the test statistic for the data with no damage is larger than the test statistic for 99 percent of the baseline data (99 percent on-sided confidence interval) then that frequency range is assumed to be unusable for damage detection in this study. The undamaged measurements indicate such an interval has too high a likelihood of false positives.

This study had relatively high rates of false positives, indicating that the variance of the data was estimated too narrowly. A primary cause of this is most likely again the assumption of independence of each data point. However, since the same assumptions were made for each frequency range, the results can still be compared across frequency ranges. If waiting for a relatively larger damage size is acceptable, the threshold level may be increased, thus reducing the number of false positives, and the more sensitive frequency ranges may be used. Complete results for each

frequency range and damage location are shown in Fig. 14 and 15 for the small and large MFC's respectively.

It is interesting to observe that for the large MFC the test statistic actually increases on average as the damage location moves further away from the sensor location. This is due to differences in the variability of the baseline damage metric. Since separate sets of baseline measurements were used for each damage location, the variability changed for each set of damage location. This indicates that the data is non-stationary. Since stationarity is a relative term, this is not an indication of any problem with the impedance method; only that in the future data should be taken for a longer period of time. Additional variability is also thrown into the analysis since the amounts of damage for different nominal values of damage can not be exactly reproduced. Regardless, the frequency range to frequency range comparisons within each damage location still remain valid, which is the primary concern of this study.

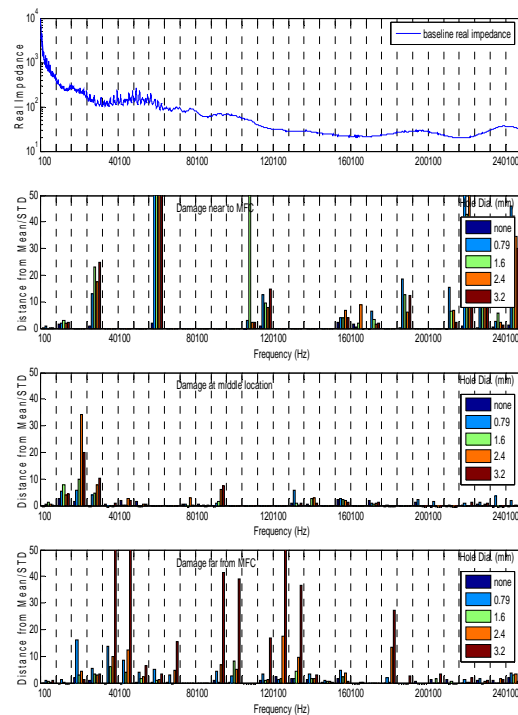


Figure 14. Damage metrics of each frequency range for the small MFC at each damage location.

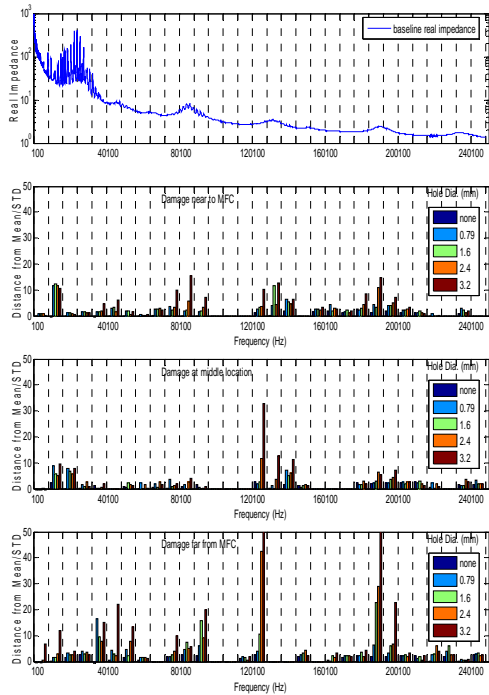


Figure 15. Damage metrics of each frequency range for the large MFC at each damage location.

Since it is already clear which frequency ranges are better predictors of damage, comparing the large MFC to the small MFC is not as useful for determining frequency ranges in this experiment compared to the aluminum beam experiment. One interesting observation though is that at the frequency ranges where the small MFC could identify damage, the test statistic was significantly higher for near field damage than the test statistic of the large MFC. The large MFC did a better job of identifying far field damage.

### Conclusions

The aim of this paper is to address the issue of which frequency ranges are best for structural health monitoring using the impedance method. In the past, the ranges are generally selected by trial and error, which often involves inducing a removable amount of simulated damage. Sensitivity analysis of frequency ranges has been performed by few previous researchers; however, since the results have not been compared to features in the impedance measurement, the study would need to be performed for each new structure tested.

Several experiments on two very different types of structures were used to examine the frequency range selection for impedance-based SHM. The frequency ranges that include the resonances of the sensor/actuators are, in

general, more suitable frequency ranges to monitor for damage identification. This corroborates with testing at frequency ranges with high modal density. Their variation is less than frequency ranges without a PZT or MFC resonance, but are more responsive to damage. The actuator resonances can be predicted through models such as the Liang's impedance model, or by measuring the response before bonding. The large MFC attached to the composite boom has the clearest results in this series of tests. The resonant peaks in the unbonded condition are spaced at a regular interval and also show up clearly in the bonded response. In cases where the actuator resonances are not as evident once bonded, the results indicate the PZT resonance still affect the sensing ability, though to a lesser extent.

The experiments also highlight the advantages of monitoring at high frequency ranges. In the aluminum beam experiment the damage metric is sensitive to damage at high frequency ranges even with changing conditions, in this case mass variability. Also with the composite boom, the higher frequency ranges were more effective at distinguishing various levels of damage.

Frequency range selection was not studied in the presence of large temperature range variations. Unlike adding a mass to induce increased variability, this would change properties not just of the structure, but also of the sensor/actuator. This potentially could cause a shift in the PZT or MFC resonant peak. If such was the case, then even though this test suggests that frequency ranges with peaks due to the sensor/actuator do have better sensing ability, these ranges may need to be avoided. This, however, would need additional testing than what was performed in this study to be verified. Other potential investigations could include size of frequency range and number of points in a frequency range.

### Acknowledgements

The authors are grateful for the support of the G.R. Goodson Professorship and NASA through the GRSP Fellowship program. The inflatable rigidizable boom was kindly provided by David P. Cadogan and Stephen E. Scarborough, of ILC Dover., Inc. The authors would also like to thank G. Eddie Simmers for creating the data acquisition program and Dr. W. Keats Wilkie for assistance with this research.

## References

- [1] Liang, C., Sun, F. and Rogers, C.A., 1994a, "Coupled Electromechanical Analysis of Adaptive Material System: Determination of Actuator Power Consumption and System Energy Transfer," *Journal of Intelligent Material Systems and Structures*, 5, pp. 12-20.
- [2] Liang, C., Sun, F., and Rogers, C., 1994b "An Impedance Method for Dynamic Analysis of Active Materials Systems," *Journal of Vibration and Acoustics*, 116, pp. 121-128.
- [3] Sun, F., C. Liang and C. A. Rogers, 1994, "Structural Modal Analysis Using Collocated Piezoelectric Actuators/Sensors: An Electromechanical Approach," *Proc. Smart Structures and Materials 1994: Smart Structures and Intelligent Systems*, 2190, pp. 238-249.
- [4] Park, G., Sohn, H., Farrar, C., and Inman, D., 2003, "Overview of Piezoelectric Impedance-Based Health Monitoring and Path Forward." *The Shock and Vibration Digest*, 35(6), pp. 451-463.
- [5] Sun, F., Chaudhry, Z., Liang, C. and Rogers, C.A. 1995, "Truss Structure Integrity Identification Using PZT Sensor-Actuator," *Journal of Intelligent Material Systems and Structures*, (6) pp. 134-139.
- [6] Park, G., Cudney, H., and Inman, D. J., 2000, "Impedance-based Health Monitoring of Civil Structural Components," *ASCE/Journal of Infrastructure Systems*, 6(4), pp. 153-160.
- [7] Giurgiutiu, V., Zagrai, A. and Bao, J.J., 2002, "Piezoelectric Wafer Embedded Active Sensors for Aging Aircraft Structural Health Monitoring", *Structural Health Monitoring*, 1(1) pp. 41-61.
- [8] Berman, J., Quattrone, R., Averbuch, A., Lalonde, F., Cudney, H., Raju, V., and Cohen, G.L., 1999, "Piezoelectric Patch Sensors for Structural Integrity Monitoring of Composite-Upgraded Masonry and Concrete Structures," US Army Corps of Engineers, Construction Engineering Research Laboratory, CERL Technical Report 99/72.
- [9] Peairs, D.M., Grisso, B.L., Inman, D.J., Page, K.R., Athman, R. and Margasahayam, R.N., 2003, "Proof-of-Concept Application of Impedance-Based Monitoring on Space Shuttle Ground Structures," NASA-TM-2003-211193.
- [10] Worden, K., Allen, D., W., Sohn, H. Stinematos, D.W., Farrar, C.R., 2002, "Extreme Value Statistics for Damage Detection in Mechanical Structures." Los Alamos National Laboratory Report LA-13905-MS. available at <http://www.lanl.gov/projects/ncsd/publications.htm>.
- [11] Todd, M., Trickey, S., Nichols, J. and Seaver, M., 2001, "Implementing Statistical Process control Methods for the Assessment of Damage in a Simple Plate Structure," *Proceedings of the 3<sup>rd</sup> International Workshop on Structural Health Monitoring: The Demands and Challenges*, Stanford, CA, 1249-1258.
- [12] Gyekenyesi, A.L., Martin R.E., Sawicki, J.T. and Baaklini, G.Y., 2005, "Damage Assessment of Aerospace Structural Components by Impedance Based Health Monitoring," NASA-TM-2005-213579.
- [13] Simmers, G.E., 2005, "Impedance-Based Structural Health Monitoring to Detect Corrosion," Master's Thesis, Virginia Polytechnic Institute and State University.
- [14] Nokes, J. and Cloud, G., 1993, "The Application of Interferometric Techniques to the Nondestructive Inspection of Fiber Reinforced Materials," *Experimental Mechanics*, 33(4), pp. 314-319.
- [15] Pohl, J., Herold, S., Mook, G., Michel, F., 2001, "Damage Detection in Smart CFRP Composites Using Impedance Spectroscopy," *Smart Materials and Structures*, 10, pp. 834-42.
- [16] Bois, C., and Hochard, C. "Measurement and Modeling for the Monitoring of Damaged Laminate Composite Structures," *Proceedings of the First European Workshop on Structural Health Monitoring*, pp. 425-432.
- [17] Grisso, B., Peairs, D., Inman, D., "Impedance-based Health Monitoring of Composites," *Proceedings of International Modal Analysis Conference (IMAC) XXII Dearborn, MI Jan. 26-29, 2004.*
- [18] Grisso, B., Peairs, D., Inman, D., 2004. "Detecting Damage in Graphite/Epoxy Composites Using Impedance-based Structural Health Monitoring," *Applied Mechanics and Materials*, 1-2, pp. 185-190.

- [19] Tarazaga, P.A., Wilkie, W.K., and Inman, D.J., 2006, "Structural Health Monitoring of Space Rigidizable-Inflatable Booms," Proceedings of International Modal Analysis Conference (IMAC) XXIV, January 30-February 2, St. Louis, MO.
- [20] Wilkie, W.K., Bryant, R.G., High, J.W., Fox, R.L., Hellbaum, R.F., Jalink, A. Jr., Little, B.D., Mirick, P.H., 2000, "Low-Cost Piezocomposite Actuator for Structural Control Applications," Proceedings, SPIE's 7th International Symposium on Smart Structures and Materials, March 5-9, Newport Beach, California.
- [21] Harrah, L., Hoyt, A., Haight, A., E., Sprouse, M., R., Allred, R., E., McElroy, P., M., Scarborough, S., and Dixit, A., 2004. Proceedings, 45th AIAA/ASME/ASCE/AHS Structures, Structural Dynamics and Materials Conference (SDM), April 19-22, Palm Springs, CA.
- [22] Sodano, H., Park, G., Inman, D.J., 2004, "An Investigation into Performance of Macro-Fiber Composites for Sensing and Structural Vibration Applications," Mechanical Systems and Signal Processing 18 pp. 683-697.
- [23] Jenkins, C. H., ed., 2001. "Gossamer Spacecraft: Membrane and inflatable Structures Technology for Space Applications," Progress in Astronautics and Aeronautics, AIAA, 19.
- [24] Tarazaga, P. A., Inman, D. J., and Wilkie, W., Keats, 2006, "Control of Space Rigidizable-Inflatable Boom Using Macro-Fiber Composite," Proceedings of 47th AIAA/ASME/ASCE/AHS Structures, Structural Dynamics and Materials Conference (SDM), May 1-4, New Port, Rhode Island.
- [25] Bent, Aaron, A., Hagood, Nesbitt, W., 1997, "Piezoelectric Fiber Composites with Interdigitated Electrodes," Journal of Intelligent Material Systems & Structures, 8(11) pp. 903-919.
- [26] Tarazaga, P.A., Peairs, D.M., Inman, D.J., Wilkie, W.K., 2006, "Structural Health Monitoring of an Inflatable Boom on Simulated Debris/Meteorite Impact," Proceedings, SPIE's 11th International Symposium on Nondestructive Evaluation for Health Monitoring and Diagnostics, February 26-March 2, San Diego, California.
- [27] Wears, R.L., 2002, "Advanced Statistics: Statistical Methods for Analyzing Cluster and Cluster-randomized Data," Academic Emergency Medicine, 9(4) pp. 330-41.